Dysregulated hemolysin liberates bacterial outer membrane vesicles for cytosolic lipopolysaccharide sensing

Shouwen Chen[1], Dahai Yang[1,2], Ying Wen[1], Zhiwei Jiang[1], Lingzhi Zhang[1,3], Jiatiao Jiang[1], Yaozhen Chen[4], Tianjian Hu[1], Qiyao Wang[1,2], Yuanxing Zhang[1,2], Qin Liu[1,2,5]*

1 State Key Laboratory of Bioreactor Engineering, East China University of Science and Technology, Shanghai, China, 2 Shanghai Engineering Research Center of Maricultured Animal Vaccines, Shanghai, China, 3 Department of Pathology and Comprehensive Cancer Center, University of Michigan, Ann Arbor, Michigan, United States of America, 4 Department of Transfusion Medicine, Xijing hospital, Xi'an, China, 5 Laboratory for Marine Biology and Biotechnology, Qingdao National Laboratory for Marine Science and Technology, Qingdao, China

* qinliu@ecust.edu.cn

Abstract

Inflammatory caspase-11/4/5 recognize cytosolic LPS from invading Gram-negative bacteria and induce pyroptosis and cytokine release, forming rapid innate antibacterial defenses. Since extracellular or vacuole-constrained bacteria are thought to rarely access the cytoplasm, how their LPS are exposed to the cytosolic sensors is a critical event for pathogen recognition. Hemolysin is a pore-forming bacterial toxin, which was generally accepted to rupture cell membrane, leading to cell lysis. Whether and how hemolysin participates in non-canonical inflammasome signaling remains undiscovered. Here, we show that hemolysin-overexpressed enterobacteria triggered significantly increased caspase-4 activation in human intestinal epithelial cell lines. Hemolysin promoted LPS cytosolic delivery from extracellular bacteria through dynamin-dependent endocytosis. Further, we revealed that hemolysin was largely associated with bacterial outer membrane vesicles (OMVs) and induced rupture of OMV-containing vacuoles, subsequently increasing LPS exposure to the cytosolic sensor. Accordingly, overexpression of hemolysin promoted caspase-11 dependent IL-18 secretion and gut inflammation in mice, which was associated with restricting bacterial colonization in vivo. Together, our work reveals a concept that hemolysin promotes noncanonical inflammasome activation via liberating OMVs for cytosolic LPS sensing, which offers insights into innate immune surveillance of dysregulated hemolysin via caspase-11/4 in intestinal antibacterial defenses.

Author summary

Sensing of lipopolysaccharide (LPS) in the cytosol triggers non-canonical inflammasome-mediated innate responses. Recent work revealed that bacterial outer membrane vesicles (OMVs) enables LPS to access the cytosol for extracellular bacteria. However, since

intracellular OMVs are generally constrained in endosomes, how OMV-derived LPS gain access to the cytosol remains unknown. Here, we reported that hemolysin largely bound with OMVs and entered cells through dynamin-dependent endocytosis. Intracellular hemolysin significantly impaired OMVs-constrained vacuole integrity and increased OMV-derived LPS exposure to the cytosolic sensor, which promoted non-canonical inflammasome activation and restricted bacterial gut infections. This work reveals that dysregulated hemolysin promotes non-canonical inflammasome activation and alerts host immune recognition, providing insights into the more sophisticated biological functions of hemolysin upon infection.

Introduction

The host innate immune system can sense invading bacteria by detecting pathogen-associated molecular patterns (PAMPs) [1]. Lipopolysaccharide (LPS), a component of the outer cell membrane of Gram-negative bacteria, is one of the strongest immune activators [2]. Extracellular and endocytosed LPS is recognized by the transmembrane protein Toll-like receptor 4 (TLR4), leading to gene transcriptional regulation in response to infection [3]. Recent studies showed that host can detect LPS in the cytosol via a second LPS receptor, caspase-11 in mice and caspase-4/5 in humans [4–6]. Caspase-11/4/5 directly binds cytosolic LPS [6], leading to its own activation, which thus cleaves gasdermin D to induce pyroptotic cell death and activate non-canonical activation of NLRP3 to release interleukin-1β (IL-1β) or IL-18 [7–8]. Therefore, compartmentalization of LPS receptors within cells allows host to respond differentially and sequentially to LPS at distinct subcellular locales, which function in concert to constitute host noncanonical inflammasome defenses.

Caspase-11/4/5, as cytosolic sensors, only recognize LPS that has entered the host cell cytoplasm; however, the mechanism by which LPS from invading bacteria gains access to the cytosolic sensors remains unclear. For intracellular bacteria, although some bacteria such as *Burkholderia* [9] are cytoplasm-residing and easily expose LPS to the cytosolic sensors, many other bacteria such as *Salmonella typhimurium* [10] or *Legionella pneumophila* [11] are predominantly constrained in pathogen-containing vacuoles (PCVs), probably masking LPS from cytosolic innate sensing. In addition to vacuolar bacteria, many extracellular bacteria, including *Escherichia coli* [12], *Vibrio cholerae* [13], *Citrobacter rodentium* [14], and *Haemophilus influenzae* [15] are thought to rarely access the cytoplasm, but induce caspase-11 dependent pyroptosis and cytokine release in cells. Thus, LPS entry into cell cytoplasm is a critical event for recognition of vacuolar or extracellular bacteria by non-canonical inflammasome. Accumulating data suggest vacuolar bacteria may shed their LPS from endosome into the cytosol [16]. Lipopolysaccharide-binding protein (LBP) is also implicated in facilitating intracellular LPS delivery [17]. Alternatively, mouse guanylate-binding protein 2 (mGBP2) induces lysis of PCVs and promotes LPS leakage into the cytoplasm [14,18–19]. Recently, Vijay A.K. Rathinam and his colleagues explored how non-canonical inflammasomes detect extracellular Gram-negative bacteria. Briefly, the outer membrane vesicles (OMVs) of extracellular bacteria enter cells by dynamin-dependent endocytosis, enabling LPS to access the cytosol by escaping from early endosomes [20]. However, how OMVs gain access from early endosomes to the cytosol remains unknown.

Hemolysin belongs to the pore-forming protein family, rupturing the cell membrane and leading to cell lysis at high doses [21]. Recently, hemolysin was found to participate in modulating cell death pathways at sublytic concentrations [21–23], representing more sophisticated

toxin activity in contrast to outright pore-forming function. Uropathogenic *Escherichia coli* (UPEC) isolate CP9 activates caspase-3/7 and stimulates rapid cell apoptotic death in vitro; this phenotype was lost in a Δ*hlyA* mutant [24], indicating the involvement of hemolysin in the cell apoptosis pathway. Recently, increasing evidence suggests that hemolysin promotes activation of inflammasome signals during infection. For example, entero-hemolysin of enterohemorrhagic *E. coli* (EHEC) O157:H7 triggered mature IL-1β secretion in human macrophages [25], and α-hemolysin of UPEC CFT073 mediated NLRP3-dependent IL-1β secretion in mouse macrophages [26]. Strikingly, overexpression of hemolysin in UPEC UT189 activated significantly increased caspase-4 dependent cell death and IL-1α release than the controls [27]. This is the first evidence demonstrating the relevance of hemolysin in caspase-4 activation, indicating that hemolysin might contribute to non-canonical inflammasome activation.

In this study, we first demonstrated that hemolysin in various enterobacteria significantly promoted caspase-4 dependent pyroptosis and IL-18 secretion in human intestinal epithelial cell lines. Further, we provided insights into the mechanism of hemolysin-mediated increase in the sensitivity of non-canonical inflammasome to invading bacteria. We showed that hemolysin internalizes into cells via binding to OMVs and promotes rupture of OMV-containing vesicles, thereby releasing OMV-derived LPS into the cytoplasm and eventually triggering significant activation of non-canonical inflammasomes in cells. Oral infection of mice showed that abnormal expression of hemolysin in vivo alerts the immune system and induces caspase-11-dependent enterocyte pyroptosis and IL-18 secretion, which significantly constrains bacterial infection in the gut. Collectively, our results reveal that overproduced hemolysin enables OMV-mediated LPS cytosolic delivery for caspase-11/4 sensing, which alarms intestinal innate immune surveillance in vivo, providing insights into the manipulation of non-canonical inflammasome signals by invading bacteria.

Results

Hemolysin promotes caspase-4 dependent cell death and IL-18 secretion during infection

To screen for bacterial factors involved in regulating non-canonical inflammasome activation, a gene-defined mutant library of *Edwardsiella tarda* (*E. tarda*), an enteric pathogen infecting hosts from fish to human [28–29], was used to identify mutants that induced significantly increased pyroprosis in HeLa cells. Compared to the wild-type strain (EIB202), one of the mutants (0909I) greatly increased LDH release (Figs S1A and 1A) and IL-18 secretion (Fig 1B), accompanied by significantly induced caspase-4 activity (Fig 1C) in HeLa. To explore whether 0909I promotes caspase-4-dependent non-canonical inflammasome activation in human intestinal epithelial cell lines., we extended the bacterial infection experiments to the wild-type and *Caspase-4*$^{-/-}$ Caco-2 and HT-29 cells. Robust pyroptosis (Figs 1D and S1B) and significantly increased LDH release (Figs 1E and S1C) and IL-18 secretion (Figs 1F and S1D) were detected in wild-type cells infected with 0909I compared to those infected with EIB202, which were abrogated in *Caspase4*$^{-/-}$ cells. These data indicate that *E. tarda* mutant 0909I promotes caspase-4 dependent inflammasome activation in non-phagocyte cells.

Next, bioinformatics analysis revealed that the transposon insert site within 0909I is located upstream of a non-RTX hemolysin-encoding gene, *ethA* [29]. In agreement with the upregulated transcription level of *ethA* (S2A Fig), 0909I showed higher EthA expression (S2B Fig) and bacterial hemolytic activity (S2C Fig) than EIB202, which were abolished in the strain of 0909IΔ*ethA*. Further, deletion of *ethA* significantly impaired the ability of 0909I to increase caspase-4 activation in Caco-2 (Fig 1D–1F) and HT-29 cells (S1B–S1D Fig). These data suggest
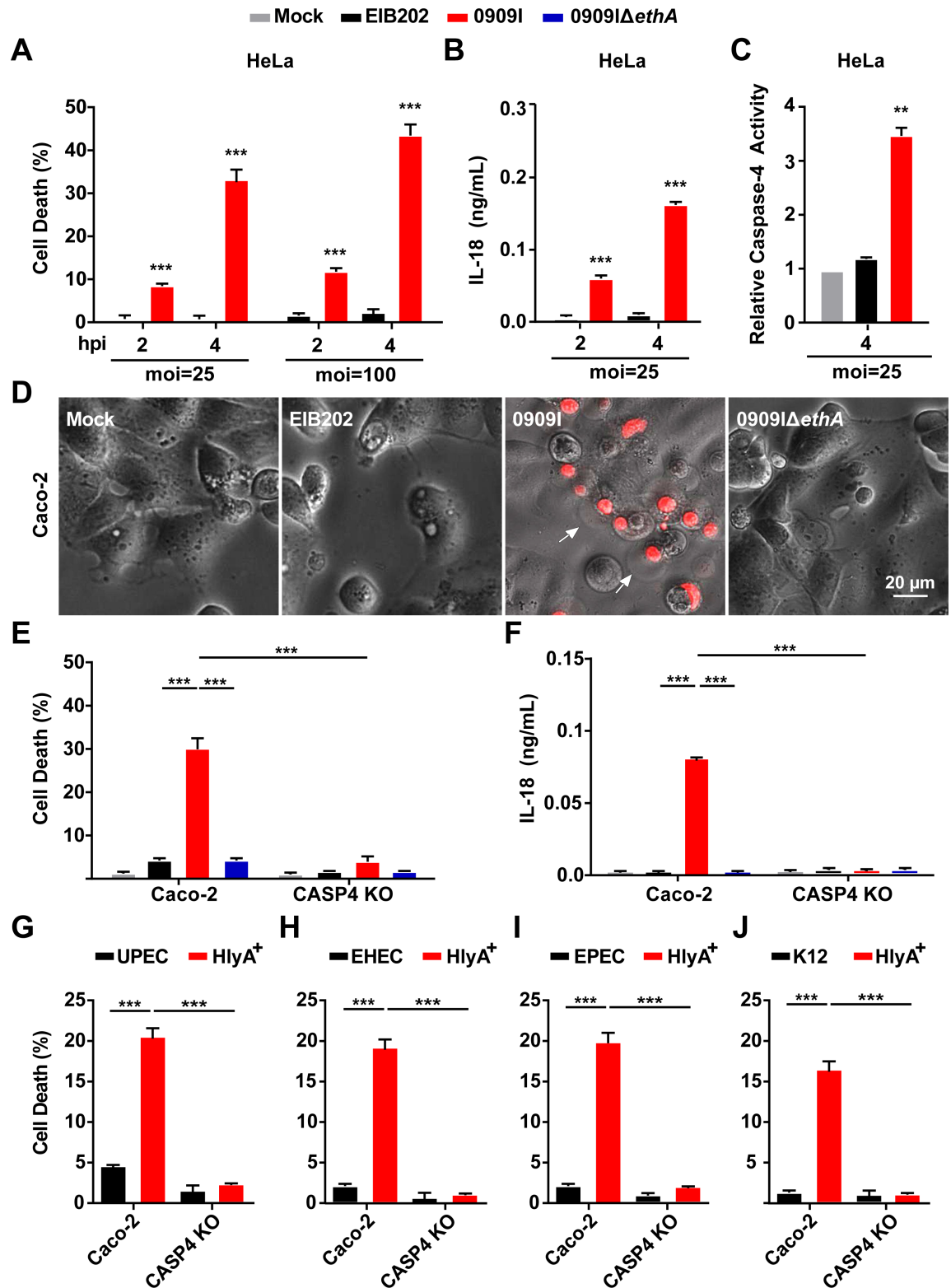
Fig 1. Hemolysin-overexpressed strains promotes caspase-4 activation during infection. (**A-B**) LDH release (A) and IL-18 secretion (B) detected in wild-type HeLa cells infected with indicated *E. tarda* strains (MOI = 25 or 100) for the indicated time periods. (**C**) caspase-4 activity measured in wild-type HeLa cells infected with indicated *E. tarda* strains (MOI = 25 or 100) for the indicated time periods, using AC-LEVD-*p*NA reagent as the assay substrate. (**D**) Cell morphology with propidium iodide (PI) staining of wild-type

Caco-2 cells infected with the indicated *E. tarda* strains (MOI = 25, 4 hpi). Scale bar, 20 μm; arrows, pyroptotic cells. (**E-J**) LDH release or IL-18 secretion detected in wild-type and *Caspase-4*^{−/−} Caco-2 cells infected with the indicated *E. tarda* (MOI = 25, 4 hpi) (E and F) or *E. coli* strains (MOI = 50, 4 hpi) (**G-J**). Graphs show the mean and s.e.m. of triplicate wells and are representative of three independent experiments. *p < 0.05, **p < 0.01, ***p < 0.001; NS, not significant (two-tailed t-test).

https://doi.org/10.1371/journal.ppat.1007240.g001

that 0909I promotes non-canonical inflammasome activation by increasing hemolysin expression.

To explore whether hemolysin also upregulates non-canonical inflammasome activation in other enteric bacteria, we expanded the investigation to the best-known RTX hemolysin, HlyA in UPEC, enterohemorrhagic *E. coli* (EHEC), enteropathogenic *E. coli* (EPEC) and *E. coli* K12. Similarly, the *E. coli* strains, containing HlyA expression plasmid, showed significantly higher hemolytic activity (S2D Fig), which elicited a higher level of caspase-4 dependent LDH release (Fig 1G–1J) and IL-18 maturation (S3A–S3D Fig) than their corresponding wild-type strains. Together, these results suggest that hemolysin plays critical roles in promoting caspase-4 activation during Gram-negative bacterial infection.

Hemolysin promotes LPS cytoplasmic release through dynamin-dependent endocytosis

Host immunity senses bacterial LPS in the cytosol via caspase-11/4/5 [4–6]. Because extracellular LPS cannot simply diffuse across the membrane, and most Gram-negative bacteria are not cytosolic, delivery of LPS from bacteria to the cytoplasm is thus very critical for non-canonical inflammasome activation. Because our data demonstrated that hemolysin increased caspase-4 activation in intestinal epithelial cells, it is reasonable to speculate that hemolysin may promote cytosolic release of bacterial LPS during infection. We extracted the cytosol of uninfected or infected Caco2 cells using digitonin and assessed LPS levels in a limulus amebocyte lysate (LAL) assay. Digitonin is commonly used to isolate cytosol [30], and the use of an extremely low concentration of digitonin (0.005%) for a very short duration allows extraction of cytosol devoid of plasma membrane, early and late endosomes, and lysosomes [20]. The LAL assay showed that LPS was present in the cytosol of infected cells, but not in uninfected cells (Fig 2A and 2B). Significantly higher levels of cytosolic LPS was detected in 0909I-infected cells than in EIB202-infected cells, and it was greatly reduced by deletion of *ethA* in 0909 (Fig 2B). These data demonstrate that hemolysin promotes LPS delivery into the cytoplasm upon *E. tarda* infection.

Edwardsiella tarda is an intracellular pathogen that replicates within a *E. tarda*-containing vacuole (ECV) [20,31–32] and has no direct access to the cytoplasm. mGBP2-induced vacuole destabilization was reported to release vacuolar bacteria for cytosolic LPS recognition [14]. However, no bacteria were recovered by agar plating in the cytosol extracted from *E. tarda*-infected cells (S4A Fig), suggesting that hemolysin did not promote vacuole-constrained *E. tarda* to enter the cytosol. Simultaneously, comparative CFUs were detected in the residual fraction between 0909I, EIB202, and 0909I∆*ethA* (S4A Fig), indicating that hemolysin did not affect cellular uptake of *E. tarda*. Further, to discriminate that hemolysin promotes LPS release to the cytoplasm from vacuolar or extracellular bacteria, three endocytosis inhibitors, cytochalasin D (CD), 5-(N-ethhyl-n-isopropil)-amiloride (EIPA), and dynasore (Dyn) were used to inhibit the internalization of *E. tarda* in Caco-2 cells. Clearly, CD and EIPA inhibited the internalization of 0909I (S4B Fig), but did not reduce either cytoplasmic LPS release (Fig 2C) or caspase-4 activation (Figs 2D and S5A), suggesting that hemolysin-mediated LPS delivery predominantly depends on extracellular bacteria. Unexpectedly, dynasore similarly inhibited cellular uptake of *E. tarda* (S4B Fig), but significantly suppressed LPS delivery (Fig 2C) and
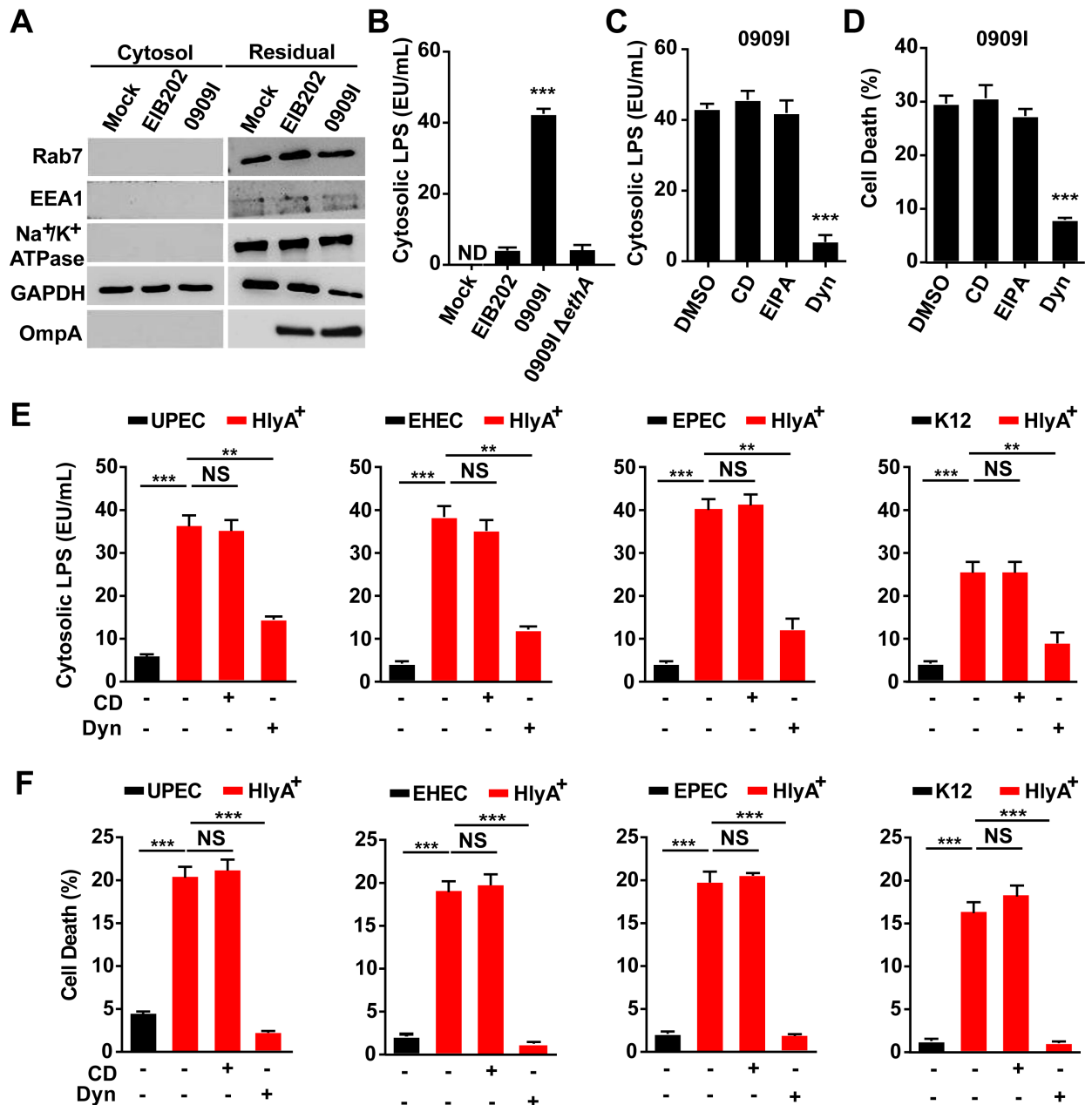
Fig 2. Hemolysin promotes LPS cytosolic release through dynamin-dependent endocytosis. (**A**) Immunoblots for Na+/K+ ATPase, EEA1, Rab7, GAPDH, and OmpA. (**B, C** and **E**) LPS quantity by LAL assay in the cytosol extracted by digitonin fractionation from *Caspase-4*^{−/−} Caco-2 cells incubated with indicated *E. tarda* strains (MOI = 25, 4 hpi) (B, C) or *E. coli* strains (MOI = 50, 4 hpi) (E) in the presence of CD (10 μM), EIPA (30 μM), Dyn (80 μM), or not. (**D, F**) LDH release detected in wild-type Caco-2 infected with indicated *E. tarda* (MOI = 25, 4 hpi) (D) or *E. coli* strains (MOI = 50, 4 hpi) (F). Graphs show the mean and s.e.m. of triplicate wells and are representative of three independent experiments. *p < 0.05, **p < 0.01, ***p < 0.001; NS, not significant (two-tailed t-test).

sensing by cytosolic caspase-4 (Figs 2D and S5A), indicating that dynasore may block a pathway that delivers LPS from extracellular bacteria to the cytoplasm. Next, we investigated the effects of CD and Dyn in *E. coli*-infected Caco-2 cells. Dyn significantly repressed LPS cytosolic release (Fig 2E), cell death (Fig 2F) and IL-18 secretion (S5B Fig) in cells, while CD showed no influence on them. These results suggest that hemolysin promotes LPS cytosolic release from extracellular bacteria through a dynamin-dependent endocytosis process.

Hemolysin-mediated caspase-4 activation is dependent on association with OMVs

Outer membrane vesicles (OMVs) are spherical, bilayered nanostructures constitutively released by growing bacteria [33]. The association of bacterial toxins with OMVs protects them from inactivation or degradation during infection, representing a highly efficient mechanism of bacteria modulating host defenses [34]. Previous studies have reported that bacterial hemolysins, such as HlyA in *E. coli* was delivered into cells via association with OMVs in a dynamin-dependent manner [22,35–37]. To dissect the role of *E. tarda* hemolysin in promoting caspase-4 inflammasome activation, we first explored the localization of EthA in this bacterium. Here, blebbing and shedding of OMVs were observed in growing *E. tarda* (S6A Fig) and produced in supernatants over time (S6B Fig). We fractionated the bacterial culture into pellets, OMV-free supernatants and OMVs. Notably, over 60% of the total EthA was detected in the fraction of OMVs (Fig 3A), indicating that OMV-associated EthA is the major form of this toxin in *E. tarda*. In accordance with the increased hemolytic activity in 0909I (S2C Fig), significantly higher levels of EthA and hemolytic activity were detected in 0909I OMVs than in EIB202 or 0909IΔ*ethA* OMVs (Fig 3B). In contrast, when subject to proteinase K (PK) digestion, in which proteins inside OMVs are protected from degradation, OMV-associated EthA was completely degraded, which agrees with the decreased hemolytic activity (Fig 3B). These data suggest that EthA is exposed on the exterior of *E. tarda* OMVs, in accord with the localization of HlyA in *E. coli* [22,36].

A recent study suggested that OMVs were responsible for delivering LPS into the cytosol and activating caspase-11 inflammasome [20]. Because *E. tarda* hemolysin was largely associated with OMVs and critically involved in caspase-4-dependent inflammasome activation, it raises the possibility that *E. tarda* employs hemolysin-associated OMVs to activate the noncanonical inflammasome during infection. Subsequently, purified *E. tarda* OMVs were incubated with wild-type or *Caspase-4*$^{-/-}$ cells. OMVs internalized and formed obvious specks within cells (S6C Fig) at comparable level between EIB202, 0909I, and 0909IΔ*ethA*, which were significantly inhibited by treatment with Dyn, but not with CD or EIPA (Fig 3C). Importantly, according to the higher hemolytic activity (Fig 3B), 0909I OMVs induced obvious cell pyroptosis (Fig 3D), and a higher level of LDH release (Fig 3F) than EIB202 OMVs in wild-type cells, and this difference was counteracted in *Caspase-4*$^{-/-}$ cells (Fig 3E). Further, hemolysin depletion by deleting *ethA* (Fig 3E) or pretreating OMVs with PK (Fig 3D) remarkably reduced 0909I OMV-induced caspase-4 activation. Simultaneously, treatment with dynasore to inhibit cellular uptake of 0909I OMVs reduced LDH release in wild-type cells (Fig 3E). Similarly, purified *E. coli* HlyA$^+$ OMVs significantly increased cell death than wild-type OMVs (Fig 3F). These data suggest that hemolysin promotes OMV-mediated caspase-4 inflammasome activation in Gram-negative bacteria.

Hemolysin impairs OMVs-containing vacuole integrity for cytosolic access of LPS

As LPS-enriched OMVs are internalized via endocytosis and restrained within endosomes [38], it raises the question of how vacuole-contained OMVs achieve cytosolic localization of LPS. Because hemolysin is a type of bacterial pore-forming toxins, that leads to membrane permeabilization [21], a possible explanation could be that hemolysin induces lysis of OMV-containing vacuoles and facilitates cytosolic exposure of LPS. Galectin-3 is a β-galactoside binding protein, that is specifically recruited to disrupted pathogen-containing vacuoles [39]. We assessed the recruitment of GFP-tagged galectin-3 in cells incubated with OMVs. Indeed, 0909I OMVs induced more galectin-3 specks than EIB202 OMVs (Figs S7A and 4A), and
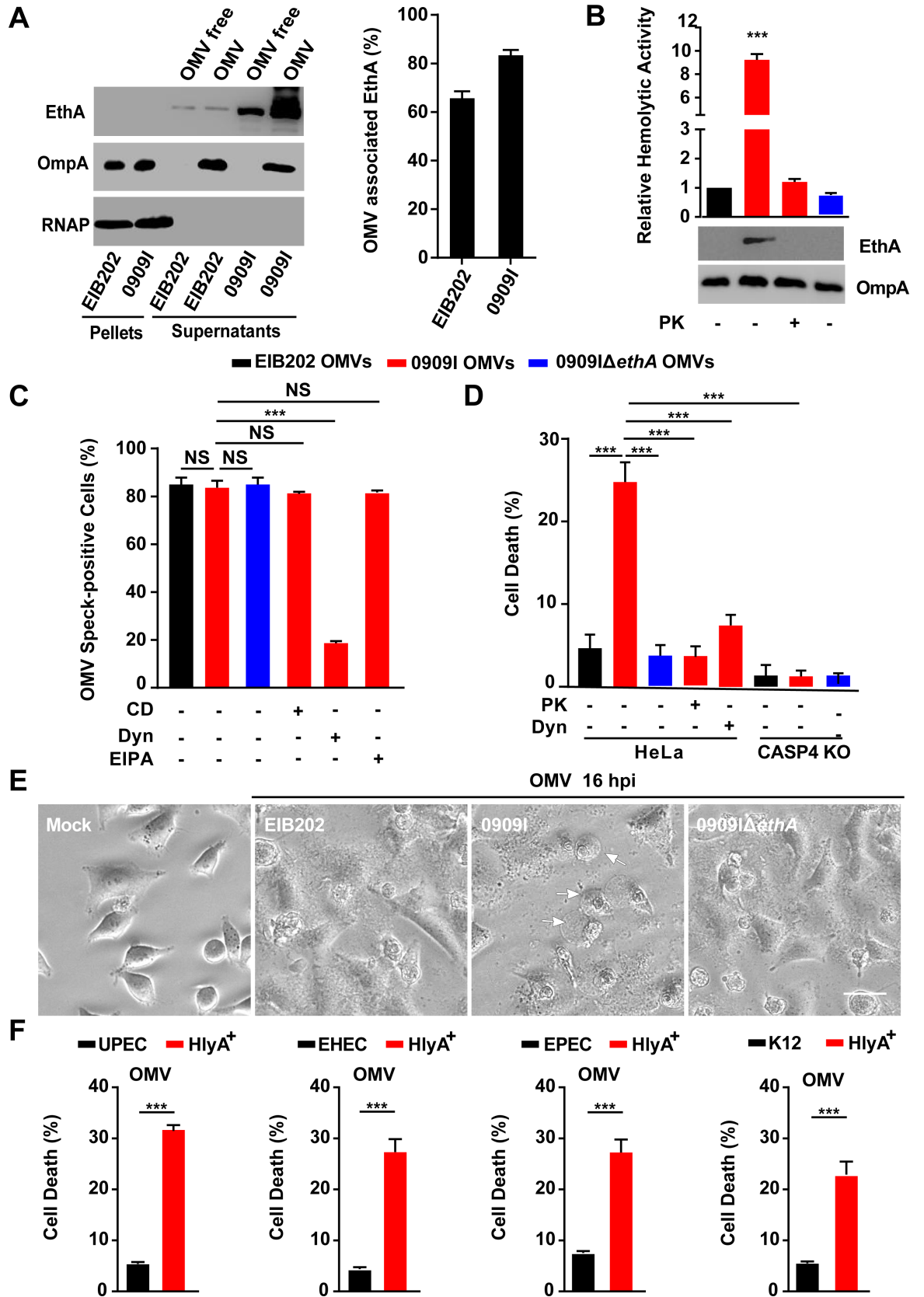
Fig 3. Hemolysin associates with OMVs to promote caspase-4 activation. (**A-B**) Immunoblots for EthA in different fractions of *E. tarda* culture at 10 h post-inoculation (A) and assay for hemolytic activity and immunoblots for EthA in OMVs, treated with PK (5 μg/mL, 5 min) or not (B). (**C**) Immunostaining for intracellular OMVs using anti-OmpA antibody and quantification of OMV speck-positive cells in HeLa cells incubated with indicated *E. tarda* OMVs (20 μg, 1×10^5 cells, 4 h) in the presence of CD (10 μM), EIPA (30 μM), Dyn (80 μM), or not. Percentage of cells containing OMV specks was calculated for at least 500 cells. (**D** and **F**) LDH release detected in wild-type or *Caspase-4*$^{-/-}$ HeLa cells incubated with purified *E. tarda* OMVs (50 μg, 1×10^5 cells, 20 h) pretreated with PK (5 μg/mL, 5 min), Dyn (80 μM), or not (D), or purified *E. coli* OMVs (50 μg, 1×10^5 cells, 20 h) (F). (**E**) Morphology of HeLa cells infected with indicated *E. tarda* OMVs (50 μg, 1×10^5 cells, 16 h). Scale bar, 20 μm; arrows, pyroptotic cells. Graphs show the mean and s. e.m. of triplicate wells and are representative of three independent experiments. $^*p < 0.05$, $^{**}p < 0.01$, $^{***}p < 0.001$; NS, not significant (two-tailed t-test).

galectin-3 showed clearly association with OMV specks within wild-type cells (Fig 4B). In contrast, removal of hemolysin from 0909I OMVs by proteinase K degradation or deleting *ethA* significantly decreased the intracellular galectin specks in wild-type cells (Fig 4A). These data suggest that hemolysin promotes rupture of OMV-containing vacuoles.

Next, we explored the contribution of hemolysin to damaging the membrane of OMV-containing vacuoles during *E. tarda* infection. As expected, 0909I triggered significantly increased signal of galectin aggregation in DMSO-treated cells, compared to EIB202 or 0909I∆*ethA* (S7B and S7C Fig). In the presence of EIPA, which inhibited the internalization of bacteria, but not OMVs into cells, 0909I induced obvious cytoplasmic galectin specks (S7B and S7C Fig), indicating that 0909I-induced galectin aggregation is mainly associated with internalized OMVs rather than bacteria. Further, 0909I trigged a significant increase in cytoplasmic galectin signal, compared to EIB202 or 0909I ∆*ethA*, which was greatly suppressed by pretreating the cells with Dyn (S7B and S7C Fig). These results suggest that hemolysin contributes to the destruction of OMV-residing vesicles during bacterial infection.

Because hemolysin triggered significant membrane rupture of OMV-containing vacuoles within cells, we evaluated whether vesicle lysis facilitates LPS exposure to cytosolic sensors. We extracted the cytosol and quantified the cytosolic LPS in *Caspase-4*$^{-/-}$ cells upon incubation with purified OMVs. Although EIB202, 0909I, and 0909I∆*ethA* OMVs showed comparable LPS contents (Fig 4C) and uptake efficiencies (Fig 3C and 3D), significantly increased cytosolic LPS was detected in the cytosol of 0909I OMV-incubated cells than in the controls. This difference was remarkably reduced by either eliminating OMV-bound hemolysin or damping OMV internalization (Fig 4D). Furthermore, purified OMVs from *E. coli* strains were incubated with *Caspase-4*$^{-/-}$ cells for the cytosolic LPS assay. Accordingly, HlyA$^+$ OMVs induced more LPS release into the cytoplasm than their correspondent wild-type OMVs (Fig 4E), indicating that hemolysin promotes cytosolic release of OMV-LPS. Collectively, these data suggest that hemolysin-mediated membrane lysis of OMV-containing vacuoles represents an important means to liberate OMV-LPS for cytosolic sensing in Gram-negative bacteria.

Hemolysin increases recognition of invading bacteria by caspase-11 inflammasome in vivo

As hemolysin was verified to promote non-canonical caspase-4 inflammasome activation in intestinal epithelium cell lines, we further assessed the involvement of hemolysin in noncanonical inflammasome activation in vivo. C57BL/6 wild-type mice were orally infected with *E. tarda* strains. Compared to EIB202, 0909I showed significantly reduced bacterial burdens in the colon, cecum and lumen (Fig 5A), but not at the systemic sites (S8A Fig), indicating that that over-expressed hemolysin restricts *E. tarda* colonization in the mouse gut. Subsequently, it is interesting to explore the in vivo relevance of hemolysin-mediated gut infection restriction with non-canonical inflammasome activation. Caspase-11 is the murine ortholog of human caspase-4, which was reported to mediate IL-18 secretion and enterocyte pyroptosis [40–42]
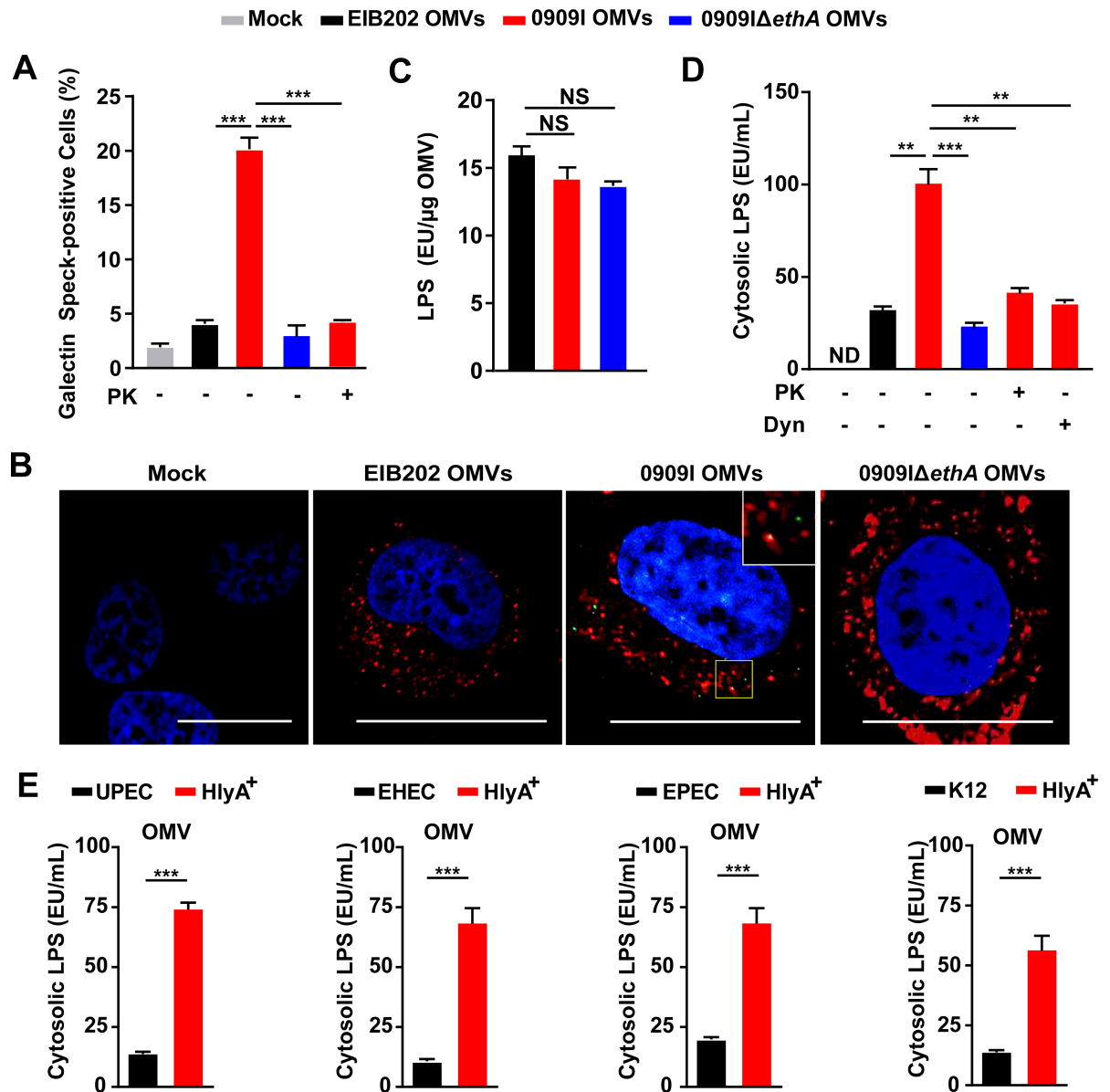
Fig 4. Hemolysin impairs OMVs-containing vacuole integrity for cytosolic access of LPS. (**A**) Quantification of galectin speck-positive cells in HeLa cells expressing GFP-tagged gelectin-3, incubated with *E. tarda* OMVs (50 μg, 1×10^5 cells, 20 h) treated by PK (5 μg/mL, 5 min) or not. Percentage of cells containing galectin specks was calculated for at least 500 cells. (**B**) Observation of intracellular galectin (green)-associated OMV specks using anti OmpA antibody (red). Scale bar, 20 μm; the white box indicates the co-localized signal between galectin and OMVs. (**C**) LPS quantification by LAL assay in purified *E. tarda* OMVs. (**D-E**) LPS quantification by LAL assay in the cytosol extracted by digitonin fractionation from *Caspase-4*^{-/-} HeLa cells, incubated with *E. tarda* OMVs (50 μg, 1×10^5 cells, 20 h) treated with PK (5 μg/mL, 5 min), Dyn (80 μM), or not (D), or *E. coli* OMVs (50 μg, 1×10^5 cells, 20 h) (E). Graphs show the mean and s.e.m. of triplicate wells and are representative of three independent experiments. *p < 0.05, **p < 0.01, ***p < 0.001; NS, not significant (two-tailed t-test).

https://doi.org/10.1371/journal.ppat.1007240.g004

during intestinal infection. Notably, caspase-11 depletion counteracted the superiority of bacterial loads in wild-type mice infected with 0909I over EIB202 (Fig 5A), suggesting the critical requirement of caspase-11 by hemolysin-triggered gut infection limitation.

Further, we demonstrated that 0909I induced remarkably higher mucosal and serum IL-18 level than EIB202 in wild-type mice (Fig 5B and 5C). Tissue pathology analysis revealed that 0909I evoked prominent intestinal inflammation in wild-type mice, typically featured by focal
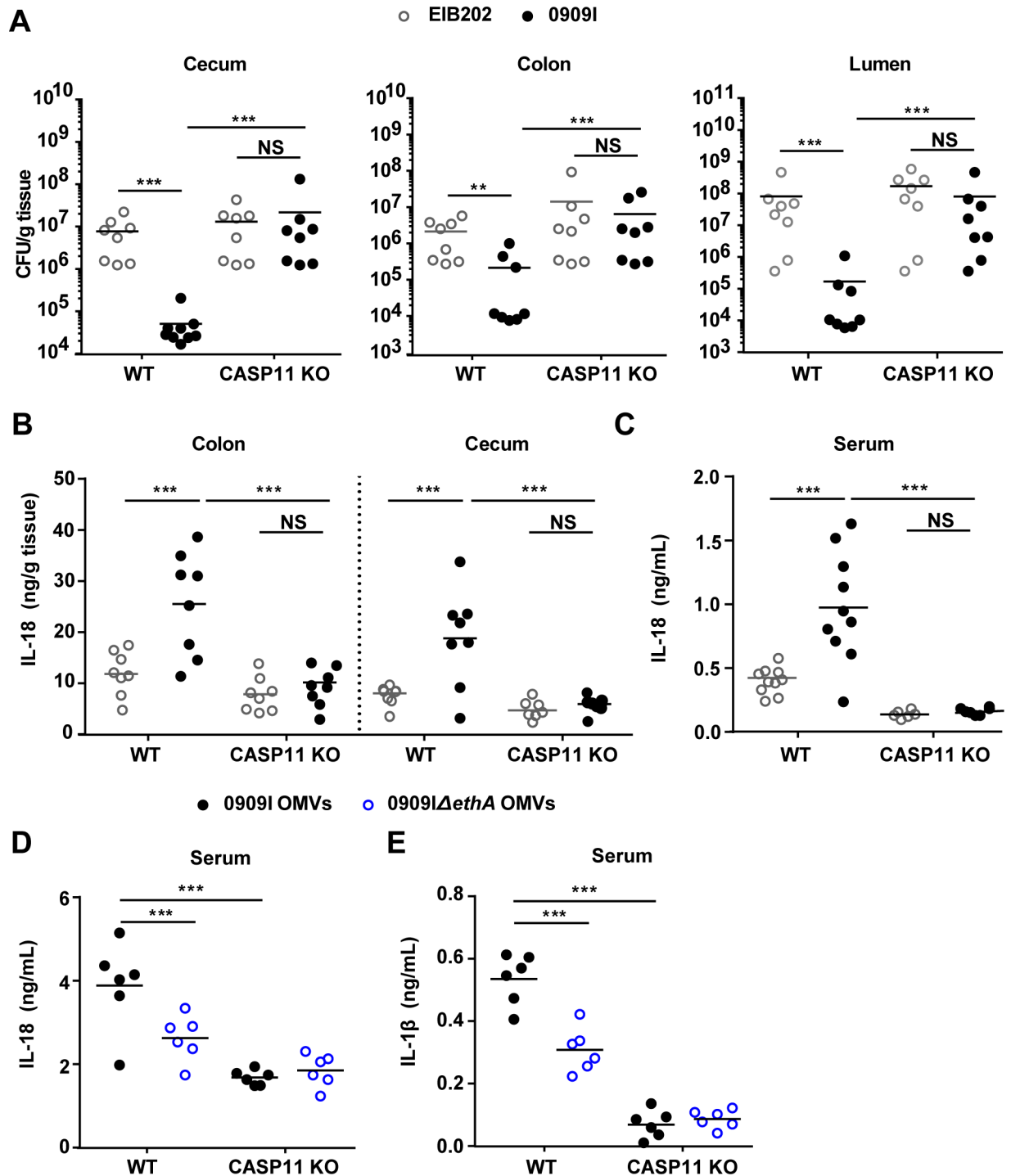
Fig 5. Hemolysin increases recognition of invading bacteria by caspase-11 in vivo. (**A**) Bacterial counting by agar plating in the colon, caecum, and lumen of wild-type or *Caspase-11*^{-/-} mice orally-infected by EIB202 or 0909I (5×10^7 cfu/g) at 24 hpi. (**B-C**) Quantification of IL-18 in the colon, cecum (B) and serum (C) of the mice described in (**A**). (**D-E**) IL-1β (D) and IL-18 (E) levels in the serum of wild-type and *Caspase-11*^{-/-} mice injected i.p. with 80 μg of OMVs. Mice were first primed with 200 mg poly(I:C) for 6 hr (i.p.). Cytokine levels were assessed 6 hr post OMV injection. Graphs depict 6–10 mice per genotype and are representative of two to three independent experiments. *p < 0.05, **p < 0.01, ***p < 0.001; NS, not significant (one-way ANOVA).

https://doi.org/10.1371/journal.ppat.1007240.g005

filtration of inflammatory cells and epithelia cell shedding (S8B and S8C Fig). Moreover, intra-peritoneally injection of 0909I OMVs caused a stronger IL-1β and IL-18 release compared with 0909IΔ*ethA* OMVs in wild-type mice (Fig 5D and 5E). In contrast, these phenotypes were largely neutralized in *Caspase-11*^{-/-} mice (Fig 5B–5E). Together, these results indicate that dys-regulation of hemolysin in vivo alerts caspase-11 dependent intestinal defenses via OMVs and restricts bacterial gut infection.

Discussion

Sensing of LPS in the cytosol by inflammatory caspase-11/4/5 has emerged as a central event of innate immune responses during Gram-negative bacterial infections [4–5,7]. Vanaja *et al.* reported that OMVs of extracellular Gram-negative bacteria can deliver LPS into the host cell cytosol from early endosomes; however, the mechanism of LPS translocation remains unclear. Biological membrane characteristics inherent to OMVs may permit them to fuse with endoso-mal membranes, leading to LPS cytosolic access [20]. Recently, it was reported that mGBPs were involved in OMV-dependent non-canonical inflammasome activation [44–45]. Mecha-nistically, mGBPs didn't promote the entry of OMVs into the cytosol, but directly target cyto-solic OMVs and facilitate the interaction of LPS with caspase-11. However, GBPs are different in mice and human due to a loss of immunity-related GTPases (IRGs) in humans, and thus hGBP2 might not have the same action as mGBP2 [46]. In addition to host factors, whether bacterial factors, such as OMV-associated bacterial components, are involved in promoting non-canonical inflammasome activation remains unknown. Here, we demonstrate that hemo-lysin binds OMVs and promotes the lysis of OMV-residing vesicles, which facilitates cytosolic release of OMV-LPS and eventually triggers significant non-canonical inflammasome signals (Fig 6). Our results suggest that hemolysin represents a biologically important mechanism for
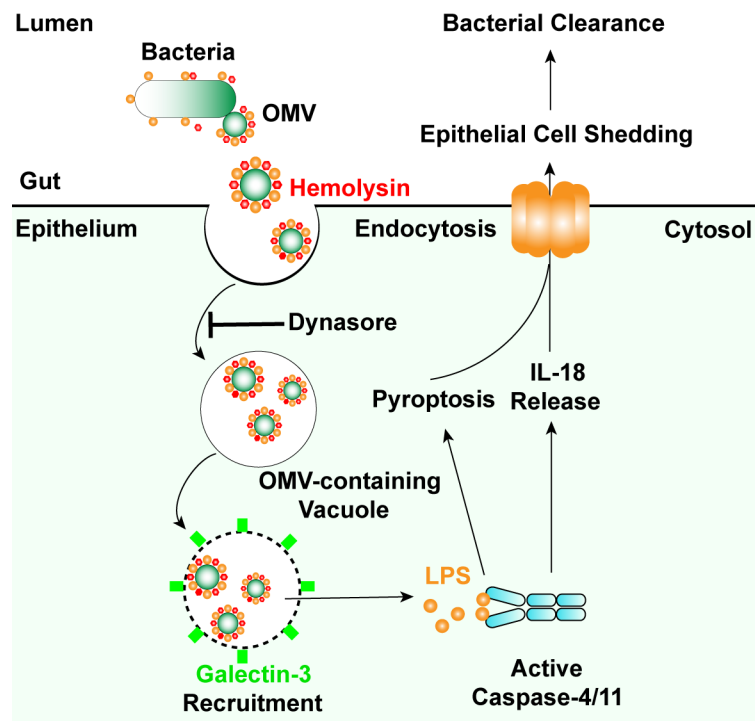

Fig 6. Model for bacterial hemolysin in regulating noncanonical inflammasome pathway. Hemolysin binds bacterial outer membrane vesicles (OMVs) and liberates OMV-associated LPS for caspase-4 sensing, which increases recognition of invading Gram-negative bacteria by non-canonical inflammasome and restricts bacterial gut infections.

https://doi.org/10.1371/journal.ppat.1007240.g006

releasing endosome-constrained OMV-LPS to cytosolic sensors. In addition to hemolysin, whether other pore-forming proteins produced by bacteria [47] play roles in liberating pathogen-associated molecular patterns for immune detection requires further examination.

Outer membrane vesicles are extruded from the surface of living bacteria and may entrap some of the underlying periplasm [33]. In addition to outer membrane proteins, LPS, phospholipids, and periplasmic constituents, OMVs deliver various bacterial cargos, including toxins intracellularly and further in specific compartments to modulate host defenses during infection [34]. Thus, OMVs offer bacterial products specific access to otherwise inaccessible cellular or tissue compartments. Particularly, OMVs enable the cytosolic localization of LPS for caspase-11 sensing [20], which is thought to be an important mechanism in extracellular bacteria. In this work, in addition to *E. coli* strains, *E. tarda*, a typical vacuolar bacterium [48] was also found to employ OMVs to activate caspase-4 with the aid of overproduced hemolysin. These results indicate that OMV-mediated non-canonical inflammasome activation represents a more generalized mechanism for bacteria than previously thought. Moreover, because OMVs were linked to the translocation of diverse bacterial factors into host cells, it will be interesting to determine whether hemolysin also increases cytosolic recognition of other ligands such as DNA or flagellin by the AIM2 [49] or NLRC4 [50] inflammasome.

Hemolysin, as a class of pore-forming toxins, is known to disrupt the membrane of eukaryotic cells at high doses in vitro, which potentially facilitates bacterial invasion and dissemination during infection [21]. HlyA is the prototype member of the hemolysin family [21]. Only a very low percentage of nonpathogenic *E. coli* harbors HlyA, while ∼50% of UPEC strains harbor and express HlyA, presenting a close correlation between increased clinic *E. coli* pathogenesis with HlyA expression [21,23,51]. In recent years, because it has been hypothesized that hemolysin is secreted at sublytic concentrations in vivo, there is increasing interest in understanding the more subtle effects of hemolysin on host cellular processes aside from outright lysis, including RhoA activation [52], Akt signaling [53], cell death pathway [22,54] and protease degradation [55]. Strikingly, *Escherichia coli* α-hemolysin toxin was reported to inhibit IL-1β secretion induced by Rho GTPase-activating toxin CNF1, thereby promoting bacterial stability in the blood [56]. Here, our study adds new findings to the scenario of hemolysin-mediated biological functions by identifying that abnormal expression of hemolysin in bacteria promotes host immune recognition of replicating pathogens via non-canonical inflammasomes and restricts bacterial colonization in vivo (Fig 6). Because hemolytic proteins exhibit multilayered or even antagonistic roles in modulating host responses to infections, it is not surprising that bacteria have evolved complicated mechanisms to fine-tune the synthesis, maturation, and transport of hemolysin [21,23,51]. Thus, studies of the spatiotemporal expression of hemolysin in vivo will be essential for understanding both host defense and bacterial survival.

Inflammasomes are activation platforms for inflammatory caspases, leading to pyroptosis and secretion of IL-1α, IL-1β, and IL-18 [15]. In contrast to the canonical inflammasome, caspase-11/4/5 mediated non-canonical inflammasome is activated by the cytosolic LPS, however, whether caspase-11/4/5 can directly cleave IL-1β or IL-18 remains controversial [41–42]. Given that the actions of inflammasomes have been well-studied in myeloid cells, accumulating evidence highlights their role in non-professional immune cells as an important antibacterial defense mechanism [43]. Recent studies demonstrated that epithelium utilize both canonical and non-canonical inflammasomes to promote mucosal defense against enteric bacterial pathogens [40–42]. These independent studies suggest that pyroptosis might lead to extrusion of infected enterocytes and promote bacterial infection in vivo even in the absence of IL-1α, IL-1β, and IL-18. In our study, hemolysin-overexpressed *E. tarda* significantly promoted caspase-11-dependent IL-18 secretion and gut inflammation in orally-infected mice.

Furthermore, intraperitoneal injection of hemolysin-rich OMVs induced higher level of serum IL-18 and IL-1β in mice than the control OMVs. These results suggest that hemolysin-associated OMVs are, if not fully, at least partially responsible for initiating Caspase-11 mediated immune defenses in vivo. Further insights into whether hemolysin-associated OMVs induces enterocyte pyroptosis and further recruits immune cells, ultimately contributing to pathogen clearance from the host, require future studies.

Materials and methods

Ethics statement

The animal trials in this study were performed according to the Chinese Regulations of Laboratory Animals—The Guidelines for the Care of Laboratory Animals (Ministry of Science and Technology of People's Republic of China) and Laboratory Animal-Requirements of Environment and Housing Facilities (GB 14925–2010, National Laboratory Animal Standardization Technical Committee). The license number associated with their research protocol was 20170912–08, which was approved by The Laboratory Animal Ethical Committee of East China University of Science and Technology. All surgery was performed under carbon dioxide anesthesia, and all efforts were made to minimize suffering.

Bacterial strains and plasmids

0909I *E. tarda* was screened from *E. tarda* gene-defined mutant library. 0909IΔ*ethA* was constructed by unmarked gene deletion. Hemolysin-overexpressing *E. coli* strains were constructed by introducing into the wild-type strain (EIB202, CCTCC M208068), the plasmid of pSF4000-*hlyBACD* [55] into UPEC UT189, EHEC EDL933 [57], EPEC (*E. coli* O26) [58] and K12, respectively.

Hemolytic activity assay

Hemolytic activity was quantified using a microtiter assay developed previously [59] with slight modifications. Indicated bacterial strains were cultured for 18–20 h and then pelleted, resuspended in PBS, and standardized at 600 nm to an OD of approximately 1.0. Next, 100 μL bacterial suspensions or OMV preparations were mixed with equal volumes of sheep erythrocytes in a 96-well plate. The plate was incubated at 37˚C with gentle shaking for the indicated time periods and erythrocytes were pelleted by centrifugation ($400 \times g$, 5 min). Clear supernatants were transferred to a fresh plate and absorbance at 540 nm was measured using a microplate reader (Dynex Technologies, Chantilly, VA, USA). Suspension buffer containing 0.1% Triton X-100 was served as a total lysis control. The percentage of hemolysis was calculated as follows: % hemolysis = (OD_{540} of samples—OD_{540} of background)/ (OD_{540} of total—OD_{540} of background) $\times$ 100.

Quantitative RT-PCR

RNA was extracted using an RNA isolation kit (Tiangen, Beijing, China). One microgram of each RNA sample was used for cDNA synthesis with the FastKing One Step RT-PCR Kit (Tiangen) and quantitative real-time PCR (RT-qPCR) was performed on an FTC-200 detector (Funglyn Biotech, Shanghai, China) using SuperReal PreMix Plus (SYBR Green) (Tiangen). The gene expression of bacterial *ethA* was evaluated for three biological replicates, and the data for each sample were expressed relative to the expression level of the 16S gene by using the $2^{-\Delta\Delta CT}$ method.

Caspase-4^{-/-} cell line establishment

sgRNA (Oligo1: GACCGGGTCATCTCTGGCGTACTCC; Oligo2: AAACGGAGTACGCCA GA GATGACCC) was designed (http://zifit.partners.org) and cloned into LentiCRISPR v2 (AddGene, Cambridge, MA, USA; 52961), containing puromycin resistance. Lentiviral particles were prepared in HEK239T cells as previously described [31]. HT-29 or Caco-2 cells were prepared in approximately 30% density and infected with lentiviral particles containing 10 μg/mL polybrene for 24 h. Transfected cells were selected with puromycin (2 μg/mL). Cells were diluted to 5 cells/mL and seeded to 96-well plates, followed by an expansion period to establish a new clonal cell line. The caspase-4^{-/-} cell lines were confirmed by western blotting using anti-caspase-4 antibody.

Cell culture and infections

Wild-type or *Caspase-4*^{-/-} Caco-2, HT-29 and HeLa cells (wild-type cells were from ATCC; F. Shao's Lab provided caspase-4 deficient HeLa cells, other deficient cells were established by our Lab) were seeded and grown to a density of $\sim 4 \times 10^5$ cells per well in 12-well plates or $\sim 10^5$ cells per well in 24-well plates. For bacterial infection, cells were incubated with indicated *E. tarda* or *E. coli* strains at a MOI of 25 or 50, respectively. Infection was initiated by centrifuging the plate at 600 ×g for 10 min. After 50-min incubation at 35˚C for *E. tarda* strains or 37˚C for *E. coli* strains, the plates were washed once with PBS and then transferred into fresh medium containing 100 μg/mL gentamicin (Gm) to kill extracellular bacteria. The time point after antibiotic treatment was recorded as 0 h after infection. For OMV infection, cells were seeded and grown to a density of $\sim 10^5$ cells per well in 24-well plates, and then incubated with purified 50 μg OMVs. Cell supernatants were harvested at the indicated time points for subsequent assays.

Cytokine and LDH release measurement

Aliquots of cellular supernatants were transferred into 96-well plates (round bottom) and centrifuged at 1000 ×g for 5 min. The supernatants were transferred to another 96-well plate (flat bottom), and the plate was subjected to the cytotoxicity assay using a CytoTox 96 assay kit (G1780, Promega, Madison, WI, USA) or an ELISA kit (eBioscience, San Diego, CA, USA) according to the manufacturer's protocol. Each sample was tested in triplicate. Cytotoxicity was normalized to Triton X-100 treatment (100% of control), and LDH release from uninfected/untreated cells was used for background subtraction.

OMV isolation

OMVs were purified from *E. tarda* strains as described previously with minor modifications [51]. Briefly, the bacterial strains were grown in 3000 mL of DMEM till OD$_{600}$ of ~1.5 and the bacteria-free supernatant was collected by centrifugation at 5000 ×*g* for 10 min at 4˚C. This supernatant was further filtered through a 0.45 μm filter and concentrated using a spin concentrator (GE Healthcare, Little Chalfont, UK; molecular weight cut off = 30 kDa). Subsequently, OMVs were pelleted by ultracentrifugation at 284100 ×*g* for 1.5 h at 4˚C in a Beckman NVT™65 rotor (Brea, CA, USA). Isolated OMVs were resuspended in PBS, transferred to the bottom of a 13-mL ultracentrifugation tube (Beckman Coulter) and adjusted to 45% OptiPrep (Sigma-Aldrich, St. Louis, MO, USA) in a final volume of 2 mL. Different OptiPrep/PBS layers were sequentially added as follows: 2 mL of 40%, 2 mL of 35%, 2 mL of 30%, 2 mL of 25% and 1 mL of 20%. Gradients were centrifuged (284000 ×*g*, 16 h, 4˚C) in a Beckman NVT™65 rotor and the fractions of equal volumes (1 mL) were removed sequentially from

the top. After removing the OptiPrep, OMVs were resuspended in 1000 μL sterile DMEM without phenol red. The protein content of purified OMVs was assessed by modified Bradford protein assay kit (Shenggong Biotech, Shanghai, China). OMV-free supernatants or OMVs, treated with proteinase K (Sigma) (5 μg/mL, 5 min) or not were separated by SDS-PAGE and immunoblotted with antibodies against OmpA, EthA, or RNAP.

OMV uptake assay

HeLa cells were seeded and grown to a density of ~7×10^4 cells per well in 24-well plates. Cells were pretreated with dyn (80 μM) or CD (1 μg/mL) for 30 min at 37˚C and incubated with 20 μg OMVs for 4 h. Cells were then washed, fixed, and quenched, and permeabilized/blocked with PBS containing 1 mg/mL saponin 10% and goat serum. OMVs were stained with anti-OmpA antibody and Alexa Fluor 488-conjugated goat anti-rabbit IgG. Actin was counter-stained with TRITC phalloidin (Yeasen Biotech, Shanghai, China) and nuclei with DAPI (Beyotime, Jiangsu, China). Fixed samples were observed under a confocal microscope (Nikon, Tokyo, Japan; A1R).

Galectin assay

The eukaryotic expression plasmid for GFP tagged galectin-3 was constructed and introduced into HeLa cells by lentivirus transfection [51]. Briefly, HeLa cells were seeded in 24-well plates at a density of 5×10^4 cells per well in antibiotic-free medium and transfected with lentiviral particles for 24 h. Next, positively-transfected cells were pooled via treating cells with 1.5 μg/mL of puromycin. The pooled cells were seeded and grown to a density of ~10^5 cells per well in 24-well plates. For bacterial infection, transfected cells were preincubated with EIPA (30 μM) or Dyn (80 μM) for 1 h before infection (DMSO pre-treatment as a control) and then challenged with different *E. tarda* strains at an MOI of 50. After 2.5 h-incubation at 35˚C, the specks of galectin recruitment were observed under a confocal microscope (Nikon, A1R). For OMV infection, cells were incubated with purified OMVs at 50 μg/10^5 cells. After 16-h incubation, the cells were washed twice with sterile PBS and fixed with 4% paraformaldehyde (PFA) at 25˚C for 2 h, then washed in PBS and permeabilized with Triton X-100 (0.1% in PBS, 10 min at 25˚C), and blocked in 5% bovine serum albumin. After overnight incubation with OmpA antibody, the cells were incubated with secondary fluorescent antibody for 1 h and DAPI was used for nuclear counterstaining. Fixed samples were observed under a confocal microscope (Nikon, A1R)

Cytosol extraction and LPS quantification

Subcellular cell fractions were extracted by a digitonin-based fractionation with modifications [30]. Briefly, *Caspase-4*$^{-/-}$ HeLa or Caco2 cells post incubation with indicated strain or purified OMVs were washed with sterile cold PBS 6 times on a platform shaker on ice to remove attached bacteria or OMVs. Subsequently, 250 or 100 μL of 0.005% digitonin extraction buffer was added to the bacteria-incubated cells in 12-well plates or OMV-incubated cells in 24-well plates, respectively. After 8 min, the supernatants were collected by centrifugation as the fraction containing cytosol, and the residuals were resuspended in 250 or 100 μL of 0.1% CHAPS buffer, respectively, as the fraction containing cell membrane, organelles and nucleus. Cytosol and residual fractions were subjected to the Limulus Amebocyte Lysate (LAL) assay (Associates of Cape Cod, East Falmouth, MA, USA) according to the manufacturer's instructions to quantify LPS.

Mice and infections

C57BL/6J wild-type and *Caspase-11*^{-/-} mice from Jackson Lab (6–8 weeks old) were bred under specific pathogen-free conditions. For oral infections, water and food were withdrawn 4 h before per os (p.o.) treatment with 20 mg/100 µL streptomycin per mouse. Afterward, animals were supplied with water and food ad libitum. At 20 h after streptomycin treatment, water and food were withdrawn again for 4 h before the mice were orally infected with 5×10^7 CFU/g of EIB202 or 0909I suspension in 200 µL PBS, or treated with sterile PBS (control). Thereafter, drinking water ad libitum was offered immediately and food 2 h post-infection. At the indicated times points, mice were sacrificed and the tissue samples from the intestinal tracts, kidneys, spleens, and livers were removed for analysis. For OMV infection, ten to 12-week-old C57BL/6 and *Caspase-11*^{-/-} mice were primed with intraperitoneal (i.p.) administration of 200 µg of poly(I:C) (high molecular weight; InvitroGen) for 6 hr prior to i.p. injection with 80 µg of purified OMVs. Cytokine levels in the serum were analyzed at 6 hr post-OMV injection [20].

Bacterial counts and histopathology analysis

Collected tissues or organs were homogenized in PBS (pH 7.4) and the dilutions were plated on Deoxycholate Hydrogen Sulfide Lactose (DHL) agar plates for CFU counting. The cecum and colon were collected in 10% neutral-buffered formalin for histological analyses. Tissue pathology was blindly scored by two researchers using hematoxylin and eosin-stained sections (6 µm). The scoring criteria for submucosal edema, PMN infiltration into the lamina propria, goblet cell loss and epithelial integrity was conducted as previously described by Barthel *et al.* [60]. In addition, inflammatory focal infiltration (IFI) within cross-section was scored at five levels (0, none; 1, inflammation occurrence, but without apparent IFI; 2, with apparent IFI; 3, more than one to three IFIs; 4, with more than three IFIs). The cumulative scoring range was 0–17.

Mucosal and serum cytokine measurements

Cecal and colonic tissues were removed from mice 24 h after infection with *E. tarda* strains. Tissues were washed free of luminal contents and then incubated in DMEM (supplemented with penicillin and streptomycin at 1% and streptomycin at 1 mg/mL) for 6 h, and the supernatants, along with the serum samples, were collected for IL-18 detection by ELISA following the manufacturer's protocols.

Antibodies

Rabbit anti-Na^{+}/K^{+} ATPase (1:1000; 3010S; Cell Signaling Technology), mouse anti-EEA1 (1:1000; ab70521; Abcam); rabbit anti-Rab7 (1;1000; ab137029; Abcam); rabbit anti-GAPDH (1:1000; 5174S; Cell Signaling Technology), rabbit anti-*E. tarda* OmpA polyclonal antibody (1:500; custom-made; Genscript Biotech, Piscataway, NJ, USA), rabbit anti-*E. tarda* EthA polyclonal antibody (1: 1000; custom-made; Genscript), and mouse anti-RNAP monoclonal antibody (1:5000; Santa Cruz Biotechnology) were used for western blotting or immunofluorescence.

Supporting information

S1 Fig. Hemolysin-overexpressing *E. tarda* strains promoted caspase-4 inflammasome activation, related to Fig 1. (A) LDH release detected in wild-type HeLa cells infected with the gene-defined mutant library of *E. tarda* at MOI = 100 for the indicated time periods, only

partial data were showed here. (**B**) Cell morphology with PI staining of HT-29 cells infected with indicated *E. tarda* strains (MOI = 25, 4 hpi), scale = 20 μm. (**C-D**) LDH release (C) and IL-18 secretion (D) detected in wild-type and *Caspase-4*^{-/-} HT-29 cells infected with indicated *E. tarda* strains (MOI = 25, 4 hpi). Graphs show the mean and s.e.m. of triplicate wells and are representative of three independent experiments. $^*p < 0.05$, $^{**}p < 0.01$, $^{***}p < 0.001$; NS, not significant (two-tailed t-test).
(TIF)

S2 Fig. Determination of hemolysin-overexpressed *E. tarda* and *E. coli* Strains, related to [Fig 1](#). (**A**) Quantitative PCR for *ethA* mRNA in *E. tarda* strains. (**B**) Immunoblots for EthA in the pellets and supernatants of *E. tarda* cultures. (**C-D**) Assay of hemolytic activity in the indicated *E. tarda* (C) or *E. coli* strains (D). Graphs show the mean and s.e.m. of triplicate wells and are representative of three (A, C and D) independent experiments. $^*p < 0.05$, $^{**}p < 0.01$, $^{***}p < 0.001$; NS, not significant (two-tailed t-test).
(TIF)

S3 Fig. Hemolysin-overexpressed *E. coli* Strains promoted IL-18 secretion in Caco-2 cells, related to [Fig 1](#). (**A-D**) IL-18 secretion detected in wild-type and *Caspase-4*^{-/-} Caco-2 cells infected with the indicated *E. coli* strains (MOI = 50, 4 hpi). Graphs show the mean and s.e.m. of triplicate wells and are representative of three independent experiments. $^*p < 0.05$, $^{**}p < 0.01$, $^{***}p < 0.001$; NS, not significant (two-tailed t-test).
(TIF)

S4 Fig. Hemolysin did not promote cellular uptake or vacuole escape of invading *E. tarda*, related to [Fig 2](#). (**A**) Bacterial count by agar plating in the cell pellets after treatment with 300 μg/mL gentamicin for 1 h to kill extracellular bacteria, or in the cytosolic fraction extracted by digitonin fractionation, both from *Caspase-4*^{-/-} Caco-2 cells infected with the indicated strains (MOI = 25, 4 hpi). (**B**) Bacterial count by agar plating in the cell pellets from *Caspase-4*^{-/-} Caco-2 cells incubated with indicated *E. tarda* 0909I (MOI = 25, 4 hpi), following treatment with 300 μg/mL gentamicin for 1 h to kill extracellular bacteria. Graphs show the mean and s.e.m. of triplicate wells and are representative of three independent experiments. $^*p < 0.05$, $^{**}p < 0.01$, $^{***}p < 0.001$; NS, not significant (two-tailed t-test).
(TIF)

S5 Fig. Effects of endocytosis inhibitors on IL-18 secretion induced by hemolysin-overexpressing strains, related to [Fig 2](#). (**A-B**) IL-18 secretion in Caco-2 cells infected by *E. tarda* 0909I (MOI = 25, 4 hpi) (A) or the indicated *E. coli* strains (MOI = 50, 4 hpi) (B), in the presence of CD (10 μM), EIPA (30 μM), Dyn (80 μM), or not. Graphs show the mean and s.e.m. of triplicate wells and are representative of three independent experiments. $^*p < 0.05$, $^{**}p < 0.01$, $^{***}p < 0.001$; NS, not significant (two-tailed t-test).
(TIF)

S6 Fig. OMVs were produced by *E. tarda* and internalized into cells, related to [Fig 3](#). (**A**) Observation of OMVs in the culture of *E. tarda* EIB202 at 10 h post-inoculation under [transmission electron microscope](#), scale = 500 nm, the white arrows indicate the OMVs. (**B**) Immunoblots for OmpA, a stably expressed outer membrane protein, in the concentrated supernatants of *E. tarda* EIB202 to roughly quantify OMVs at indicated time periods. (**C**) Immunostaining for intracellular OMV specks using anti-OmpA antibody in HeLa cells incubated with the indicated *E. tarda* OMVs (20 μg/1 × 10⁵ cells, 4 h), Scale = 20 μm.
(TIF)

S7 Fig. Recruitment of galectin-3 to disrupted OMV-containing vacuoles, related to Fig 4.
(**A**-**B**) Formation of galectin specks within HeLa cells expressing GFP-tagged gelectin-3, incubated with *E. tarda* OMVs (50 μg, 1×10^5 cells, 16 h) (A), or infected with *E. tarda* stains (MOI = 25, 4 hpi) pretreating with EIPA (30 μM), Dyn (80 μM), or not (B), scale = 20 μm, the white arrows indicate the galectin specks within cells. (**C**) Quantification of galectin speck-positive cells in the infected cells as described in (B), the percentage of cells containing galectin specks was calculated for at least 500 cells. Graphs show the mean and s.e.m. of triplicate wells and are representative of three independent experiments. $^*p < 0.05$, $^{**}p < 0.01$, $^{***}p < 0.001$; NS, not significant (two-tailed t-test).
(TIF)

S8 Fig. Bacterial loads and intestinal histopathology of orally-infected mice, related to Fig 5. (**A**) Bacterial counting by agar plating in the liver, spleen, and kidney of wild-type mice orally-infected by EIB202 or 0909I (5×10^7 cfu/g) at 24 hpi. (**B**) H&E staining of the colon and caecum sections from the mice described in A, magnification = 200 ×, the black arrows indicate the inflammatory focal infiltration (IFI). (**C**) Histological scores of the gut sections in (B). Graphs depict 6–8 mice per genotype and are representative of two independent experiments. $^*p < 0.05$, $^{**}p < 0.01$, $^{***}p < 0.001$; NS, not significant (one-way ANOVA).
(TIF)

Acknowledgments

Author Contributions

Conceptualization: Shouwen Chen, Qin Liu.

Data curation: Shouwen Chen, Ying Wen, Zhiwei Jiang, Lingzhi Zhang, Jiatiao Jiang.

Formal analysis: Shouwen Chen, Dahai Yang, Qiyao Wang, Qin Liu.

Funding acquisition: Qin Liu.

Investigation: Shouwen Chen, Qin Liu.

Methodology: Shouwen Chen, Ying Wen, Zhiwei Jiang, Lingzhi Zhang, Jiatiao Jiang, Yaozhen Chen, Tianjian Hu, Qin Liu.

Project administration: Qin Liu.

Resources: Shouwen Chen, Qin Liu.

Software: Shouwen Chen.

Supervision: Qiyao Wang, Yuanxing Zhang, Qin Liu.

Validation: Shouwen Chen.

Visualization: Shouwen Chen.

Writing – original draft: Shouwen Chen, Dahai Yang, Qin Liu.

Writing – review & editing: Dahai Yang, Qin Liu.

References

1. Vance RE, Isberg RR, Portnoy DA. (2009) Patterns of Pathogenesis: Discrimination of Pathogenic and Nonpathogenic Microbes by the Innate Immune System. Cell Host & Microbe 6: 10–21.

2. Rosadini CV, Kagan JC. (2017) Early innate immune responses to bacterial LPS. Curr Opin Immunol 44: 14–19. https://doi.org/10.1016/j.coi.2016.10.005 PMID: 27842237

3. Kagan JC, Su T, Horng T, Chow A, Akira S, et al. (2008) TRAM couples endocytosis of Toll-like receptor 4 to the induction of interferon-beta. Nat Immunol 9: 361–368. https://doi.org/10.1038/ni1569 PMID: 18297073

4. Hagar JA, Powell DA, Aachoui Y, Ernst RK, Miao EA. (2013) Cytoplasmic LPS activates caspase-11: implications in TLR4-independent endotoxic shock. Science 341: 1250–1253. https://doi.org/10.1126/science.1240988 PMID: 24031018

5. Kayagaki N, Wong MT, Stowe IB, Ramani SR, Gonzalez LC, et al. (2013) Noncanonical inflammasome activation by intracellular LPS independent of TLR4. Science 341: 1246–1249. https://doi.org/10.1126/science.1240248 PMID: 23887873

6. Shi J, Zhao Y, Wang Y, Gao W, Ding J, et al. (2014) Inflammatory caspases are innate immune receptors for intracellular LPS. Nature 514: 187–192. https://doi.org/10.1038/nature13683 PMID: 25119034

7. Shi J, Zhao Y, Wang K, Shi X, Wang Y, et al. (2015) Cleavage of GSDMD by inflammatory caspases determines pyroptotic cell death. Nature 526: 660–665. https://doi.org/10.1038/nature15514 PMID: 26375003

8. Yang J, Zhao Y, Shao F. (2015) Non-canonical activation of inflammatory caspases by cytosolic LPS in innate immunity. Curr Opin Immunol 32: 78–83. https://doi.org/10.1016/j.coi.2015.01.007 PMID: 25621708

9. Aachoui Y, Leaf IA, Hagar JA, Fontana MF, Campos CG, et al. (2013) Caspase-11 protects against bacteria that escape the vacuole. Science 339: 975–978. https://doi.org/10.1126/science.1230751 PMID: 23348507

10. Broz P, Ruby T, Belhocine K, Bouley DM, Kayagaki N, et al. (2012) Caspase-11 increases susceptibility to *Salmonella* infection in the absence of caspase-1. Nature 490: 288–291. https://doi.org/10.1038/nature11419 PMID: 22895188

11. Case CL, Kohler LJ, Lima JB, Strowig T, de Zoete MR, et al. (2013) Caspase-11 stimulates rapid flagellin-independent pyroptosis in response to *Legionella pneumophila*. Proc Natl Acad Sci U S A 110: 1851–1856. https://doi.org/10.1073/pnas.1211521110 PMID: 23307811

12. Kayagaki N, Warming S, Lamkanfi M, Vande WL, Louie S, et al. (2011) Non-canonical inflammasome activation targets caspase-11. Nature 479: 117–121. https://doi.org/10.1038/nature10558 PMID: 22002608

13. Kailasan VS, Rathinam VA, Atianand MK, Kalantari P, Skehan B, et al. (2014) Bacterial RNA: DNA hybrids are activators of the NLRP3 inflammasome. Proc Natl Acad Sci U S A 111: 7765–7770. https://doi.org/10.1073/pnas.1400075111 PMID: 24828532

14. Meunier E, Dick MS, Dreier RF, Schurmann N, Kenzelmann BD, et al. (2014) Caspase-11 activation requires lysis of pathogen-containing vacuoles by IFN-induced GTPases. Nature 509: 366–370. https://doi.org/10.1038/nature13157 PMID: 24739961

15. Rathinam VA, Fitzgerald KA. (2016) Inflammasome Complexes: Emerging Mechanisms and Effector Functions. Cell 165: 792–800. https://doi.org/10.1016/j.cell.2016.03.046 PMID: 27153493

16. Garcia-del PF, Stein MA, Finlay BB. (1997) Release of lipopolysaccharide from intracellular compartments containing *Salmonella typhimurium* to vesicles of the host epithelial cell. Infect Immun 65: 24–34. PMID: 8975888

17. Kopp F, Kupsch S, Schromm AB. (2016) Lipopolysaccharide-binding protein is bound and internalized by host cells and colocalizes with LPS in the cytoplasm: Implications for a role of LBP in intracellular LPS-signaling. Biochim Biophys Acta 1863: 660–672. https://doi.org/10.1016/j.bbamcr.2016.01.015 PMID: 26804480

18. Finethy R, Jorgensen I, Haldar AK, de Zoete MR, Strowig T, et al. (2015) Guanylate binding proteins enable rapid activation of canonical and noncanonical inflammasomes in Chlamydia-infected macrophages. Infect Immun 83: 4740–4749. https://doi.org/10.1128/IAI.00856-15 PMID: 26416908

19. Pilla DM, Hagar JA, Haldar AK, Mason AK, Degrandi D, et al. (2014) Guanylate binding proteins promote caspase-11-dependent pyroptosis in response to cytoplasmic LPS. Proc Natl Acad Sci U S A 111: 6046–6051. https://doi.org/10.1073/pnas.1321700111 PMID: 24715728

20. Vanaja SK, Russo AJ, Behl B, Banerjee I, Yankova M, et al. (2016) Bacterial Outer Membrane Vesicles Mediate Cytosolic Localization of LPS and Caspase-11 Activation. Cell 165: 1106–1119. https://doi.org/10.1016/j.cell.2016.04.015 PMID: 27156449

21. Wiles TJ, Mulvey MA. (2013) The RTX pore-forming toxin alpha-hemolysin of uropathogenic *Escherichia coli*: progress and perspectives. Future Microbiol 8: 73–84. https://doi.org/10.2217/fmb.12.131 PMID: 23252494

22. Bielaszewska M, Ruter C, Kunsmann L, Greune L, Bauwens A, et al. (2013) Enterohemorrhagic *Escherichia coli* hemolysin employs outer membrane vesicles to target mitochondria and cause endothelial and epithelial apoptosis. PLoS Pathog 9: e1003797. https://doi.org/10.1371/journal.ppat.1003797 PMID: 24348251

23. Ristow LC, Welch RA. (2016) Hemolysin of uropathogenic *Escherichia coli*: A cloak or a dagger? Biochim Biophys Acta 1858: 538–545. https://doi.org/10.1016/j.bbamem.2015.08.015 PMID: 26299820

24. Russo TA, Davidson BA, Genagon SA, Warholic NM, Macdonald U, et al. (2005) *E. coli* virulence factor hemolysin induces neutrophil apoptosis and necrosis/lysis in vitro and necrosis/lysis and lung injury in a rat pneumonia model. Am J Physiol Lung Cell Mol Physiol 289: L207–L216. https://doi.org/10.1152/ajplung.00482.2004 PMID: 15805136

25. Zhang X, Cheng Y, Xiong Y, Ye C, Zheng H, et al. (2012) Enterohemorrhagic *Escherichia coli* specific enterohemolysin induced IL-1beta in human macrophages and EHEC-induced IL-1beta required activation of NLRP3 inflammasome. PLoS One 7: e50288. https://doi.org/10.1371/journal.pone.0050288 PMID: 23209696

26. Schaale K, Peters KM, Murthy AM, Fritzsche AK, Phan MD, et al. (2016) Strain- and host species-specific inflammasome activation, IL-1beta release, and cell death in macrophages infected with uropathogenic *Escherichia coli*. Mucosal Immunol 9: 124–136. https://doi.org/10.1038/mi.2015.44 PMID: 25993444

27. Nagamatsu K, Hannan TJ, Guest RL, Kostakioti M, Hadjifrangiskou M, et al. (2015) Dysregulation of *Escherichia coli* alpha-hemolysin expression alters the course of acute and persistent urinary tract infection. Proc Natl Acad Sci U S A 112: E871–E880. https://doi.org/10.1073/pnas.1500374112 PMID: 25675528

28. Chen H, Yang D, Han F, Tan J, Zhang L, et al. (2017) The Bacterial T6SS Effector EvpP Prevents NLRP3 Inflammasome Activation by Inhibiting the Ca (2+)-Dependent MAPK-Jnk Pathway. Cell Host Microbe 21: 47–58. https://doi.org/10.1016/j.chom.2016.12.004 PMID: 28081443

29. Wang Q, Yang M, Xiao J, Wu H, Wang X, et al. (2009) Genome sequence of the versatile fish pathogen *Edwardsiella tarda* provides insights into its adaptation to broad host ranges and intracellular niches. PLoS One 4: e7646. https://doi.org/10.1371/journal.pone.0007646 PMID: 19865481

30. Ramsby M, Makowski G. (2011) Differential detergent fractionation of eukaryotic cells. Cold Spring Harb Protoc 2011: t5592.

31. Cao H, Yang C, Quan S, Hu T, Zhang L, et al. (2018) Novel T3SS effector EseK in *Edwardsiella piscicida* is chaperoned by EscH and EscS to express virulence. Cell Microbiol 20: e12790.

32. Hou M, Chen R, Yang D, Nunez G, Wang Z, et al. (2017) Identification and functional characterization of EseH, a new effector of the type III secretion system of *Edwardsiella piscicida*. Cell Microbiol 19: e12638.

33. Schwechheimer C, Kuehn MJ. (2015) Outer-membrane vesicles from Gram-negative bacteria: biogenesis and functions. Nat Rev Microbiol 13: 605–619. https://doi.org/10.1038/nrmicro3525 PMID: 26373371

34. Kaparakis-Liaskos M, Ferrero RL. (2015) Immune modulation by bacterial outer membrane vesicles. Nat Rev Immunol 15: 375–387. https://doi.org/10.1038/nri3837 PMID: 25976515

35. Horstman AL, Kuehn MJ. (2000) Enterotoxigenic Escherichia coli secretes active heat-labile enterotoxin via outer membrane vesicles. J Biol Chem 275: 12489–12496. PMID: 10777535

36. Balsalobre C, Silva´n JM, Berglund S, Mizunoe Y, Uhlin BE, et al. (2006) Release of the type I secreted a-haemolysin via outer membrane vesicles from *Escherichia coli*. Mol. Microbiol. 59: 99–112. https://doi.org/10.1111/j.1365-2958.2005.04938.x PMID: 16359321

37. Rompikuntal PK, Thay B, Khan MK, Alanko J, Penttinen AM, et al. (2012) Perinuclear localization of internalized outer membrane vesicles carrying active cytolethal distending toxin from Aggregatibacter actinomycetemcomitans. Infect Immun 80: 31–42. https://doi.org/10.1128/IAI.06069-11 PMID: 22025516

38. O'Donoghue EJ, Krachler AM. (2016) Mechanisms of outer membrane vesicle entry into host cells. Cell Microbiol 18: 1508–1517. https://doi.org/10.1111/cmi.12655 PMID: 27529760

39. Paz I, Sachse M, Dupont N, Mounier J, Cederfur C, et al. (2010) Galectin-3, a marker for vacuole lysis by invasive pathogens. Cell Microbiol 12: 530–544. https://doi.org/10.1111/j.1462-5822.2009.01415.x PMID: 19951367

40. Sellin ME, Muller AA, Felmy B, Dolowschiak T, Diard M, et al. (2014) Epithelium-intrinsic NAIP/NLRC4 inflammasome drives infected enterocyte expulsion to restrict *Salmonella* replication in the intestinal mucosa. Cell Host Microbe 16: 237–248. https://doi.org/10.1016/j.chom.2014.07.001 PMID: 25121751

41. Knodler LA, Crowley SM, Sham HP, Yang H, Wrande M, et al. (2014) Noncanonical inflammasome activation of caspase-4/caspase-11 mediates epithelial defenses against enteric bacterial pathogens. Cell Host Microbe 16: 249–256. https://doi.org/10.1016/j.chom.2014.07.002 PMID: 25121752

42. Pallett MA, Crepin VF, Serafini N, Habibzay M, Kotik O, et al. (2017) Bacterial virulence factor inhibits caspase-4/11 activation in intestinal epithelial cells. Mucosal Immunol 10: 602–612. https://doi.org/10.1038/mi.2016.77 PMID: 27624779

43. Sellin ME, Maslowski KM, Maloy KJ, Hardt WD. (2015) Inflammasomes of the intestinal epithelium. Trends Immunol 36: 442–450. https://doi.org/10.1016/j.it.2015.06.002 PMID: 26166583

44. Finethy R, Luoma S, Orench-Rivera N, Feeley EM, Haldar AK, et al. (2017) Inflammasome Activation by Bacterial Outer Membrane Vesicles Requires Guanylate Binding Proteins. MBio 8: e01188–17. https://doi.org/10.1128/mBio.01188-17 PMID: 28974614

45. Santos JC, Dick MS, Lagrange B, Degrandi D, Pfeffer K, et al. (2018) LPS targets host guanylate-binding proteins to the bacterial outer membrane for non-canonical inflammasome activation. EMBO J 37: e98089. https://doi.org/10.15252/embj.201798089 PMID: 29459437

46. Hunn JP, Feng CG, Sher A, Howard JC. (2011) The immunity-related GTPases in mammals: a fast-evolving cell-autonomous resistance system against intracellular pathogens. Mammalian genome 22: 43–54 https://doi.org/10.1007/s00335-010-9293-3 PMID: 21052678

47. Bischofberger M, Iacovache I, van der Goot FG. (2012) Pathogenic pore-forming proteins: function and host response. Cell Host Microbe 12: 266–275. https://doi.org/10.1016/j.chom.2012.08.005 PMID: 22980324

48. Zhang L, Ni C, Xu W, Dai T, Yang D, et al. (2016) Intramacrophage Infection Reinforces the Virulence of *Edwardsiella tarda*. J Bacteriol 198: 1534–1542. https://doi.org/10.1128/JB.00978-15 PMID: 26953340

49. Burckstummer T, Baumann C, Bluml S, Dixit E, Durnberger G, et al. (2009) An orthogonal proteomic-genomic screen identifies AIM2 as a cytoplasmic DNA sensor for the inflammasome. Nat Immunol 10: 266–272. https://doi.org/10.1038/ni.1702 PMID: 19158679

50. Zhao Y, Shao F. (2015) The NAIP-NLRC4 inflammasome in innate immune detection of bacterial flagellin and type III secretion apparatus. Immunol Rev 265: 85–102. https://doi.org/10.1111/imr.12293 PMID: 25879286

51. Bielaszewska M, Aldick T, Bauwens A, Karch H. (2014) Hemolysin of enterohemorrhagic *Escherichia coli*: structure, transport, biological activity and putative role in virulence. Int J Med Microbiol 304: 521–529. https://doi.org/10.1016/j.ijmm.2014.05.005 PMID: 24933303

52. Mansson LE, Kjall P, Pellett S, Nagy G, Welch RA, et al. (2007) Role of the lipopolysaccharide-CD14 complex for the activity of hemolysin from uropathogenic *Escherichia coli*. Infect Immun 75: 997–1004. https://doi.org/10.1128/IAI.00957-06 PMID: 17101668

53. Mansson LE, Melican K, Boekel J, Sandoval RM, Hautefort I, et al. (2007) Real-time studies of the progression of bacterial infections and immediate tissue responses in live animals. Cell Microbiol 9: 413–424. https://doi.org/10.1111/j.1462-5822.2006.00799.x PMID: 16953802

54. Zhang X, Cheng Y, Xiong Y, Ye C, Zheng H, et al. (2012) Enterohemorrhagic *Escherichia coli* specific enterohemolysin induced IL-1beta in human macrophages and EHEC-induced IL-1beta required activation of NLRP3 inflammasome. PLoS One 7: e50288. https://doi.org/10.1371/journal.pone.0050288 PMID: 23209696

55. Dhakal BK, Mulvey MA. (2012) The UPEC pore-forming toxin alpha-hemolysin triggers proteolysis of host proteins to disrupt cell adhesion, inflammatory, and survival pathways. Cell Host Microbe 11: 58–69. https://doi.org/10.1016/j.chom.2011.12.003 PMID: 22264513

56. Diabate M, Munro P, Garcia E, Jacquel A, Michel G, Obba S, et al. (2015) *Escherichia coli* α-Hemolysin Counteracts the Anti-Virulence Innate Immune Response Triggered by the Rho GTPase Activating Toxin CNF1 during Bacteremia. PLoS Pathog 11(3): e1004732. https://doi.org/10.1371/journal.ppat.1004732 PMID: 25781937

57. Burgos YK, Pries K, Pestana DCA, Beutin L. (2009) Characterization of the alpha-haemolysin determinant from the human enteropathogenic *Escherichia coli* O26 plasmid pEO5. FEMS Microbiol Lett 292: 194–202. https://doi.org/10.1111/j.1574-6968.2009.01496.x PMID: 19175679

58. Schmidt H, Beutin L, Karch H. (1995) Molecular analysis of the plasmid-encoded hemolysin of *Escherichia coli* O157:H7 strain EDL 933. Infect Immun 63: 1055–1061. PMID: 7868227

59. Aldick T, Bielaszewska M, Zhang W, Brockmeyer J, Schmidt H, et al. (2007) Hemolysin from Shiga toxin-negative *Escherichia coli* O26 strains injures microvascular endothelium. Microbes Infect 9: 282–290. https://doi.org/10.1016/j.micinf.2006.12.001 PMID: 17314059

60. Barthel M, Hapfelmeier S, Quintanilla-Martinez L, Kremer M, Rohde M, et al. (2003) Pretreatment of mice with streptomycin provides a *Salmonella enterica serovar Typhimurium* colitis model that allows analysis of both pathogen and host. Infect Immun 71: 2839–2858. https://doi.org/10.1128/IAI.71.5.2839-2858.2003 PMID: 12704158